RASĀYAN *J. Chem.*
Vol. 19 | No. 4 | 1948-1960 | October-December | 2026
ISSN: 0974-1496 | e-ISSN: 0976-0083 | CODEN: RJCABP
http://www.rasayanjournal.com
http://www.rasayanjournal.co.in

SYNTHESIS, ANTIMICROBIAL EVALUATION, MOLECULAR DOCKING, AND TOXICITY PREDICTION OF N-BENZYLIDENE-1,2,4-TRIAZOLO[4,3-*b*]PYRIDAZINE DERIVATIVES

N. Devika[1], M. Mariyappan[1], J.S. Ruso[2,✉] N. Sivakumar[3], and T. Anandaraja[4]
[1]Department of Chemistry, Thiru.Vi. Ka Govt. Arts College,
Thiruvarur-610003, (Tamil Nadu), India
[2]Department of Polymer Science, University of Madras, Chennai-600025, (Tamil Nadu), India
[3]Department of Chemistry, Thanthai Periyar Govt. Arts & Science College, Trichy-620023
(Tamil Nadu), India
[4]National Dope Testing Laboratory, New Delhi-110003 (Delhi), India
✉Corresponding author: rusojs@gmail.com

ABSTRACT
A total of eleven novel N-benzylidene-[1,2,4]triazolo[4,3-*b*]pyridazine derivatives (5a–5k) were synthesised and structurally characterised by ^{1}H NMR, ^{13}C NMR, and mass spectroscopy. All eleven scaffolds were screened against a panel of bacterial and fungal pathogens to assess their antimicrobial activity. Several newly synthesised derivatives possessed substantial inhibitory effects which are comparable to those of the reference drugs. Because of the extensive pharmacological potential of 1,2,4-triazole derivatives, computational docking studies were performed on all the synthesised scaffolds to investigate their binding interactions with the β-catenin protein (PDB ID: 1JDH), a therapeutically relevant molecular target involved in cancer progression. Compounds 5e, 5f, 5g, and 5h exhibited favourable binding scores similar to the reference inhibitor FH-535. To further explore, toxicity prediction using ProTox-3.0 was carried out to assess the safety profile of the selected compounds, suggesting acceptable safety limits. However, the continuous emergence of antimicrobial resistance highlights the urgent need for structurally diverse and effective antimicrobial agents. The comprehensive results based on the experimental and computational approaches revealed that these novel hybrids (5a-5k) represent promising scaffolds for the development of antimicrobial and other useful therapeutic drugs, thereby contributing to United Nations Sustainable Development Goal 3: Good Health and Well-being.
Keywords: Triazole, Pyridazine, Molecular Docking, Antibacterial Activity, Drug Discovery, Toxicity Prediction**.**
RASĀYAN *J. Chem.*, Vol. 19, No.4, 2026

INTRODUCTION

Despite the continued substantial progress in drug discovery, the urgency to explore highly efficient therapeutic substances with strong safety profiles is still in demand due to the increasing prevalence of infectious diseases, cancer, diabetes, and other chronic disorders. Among these health concerns, diseases arising from microbial resistance represent one of the major global challenges, impairing the effectiveness of currently available conventional drugs and stressing the importance of advancing structurally active biomolecules with improved therapeutic potential. Among the azole family of five-membered heterocyclic compounds, the 1,2,4-triazole scaffold has been acknowledged as a valuable structural framework in therapeutic research because of its pleiotropic medicinal properties, including antimicrobial,[1-2] antioxidant,[3] antihypertensive,[4] antineoplastic,[5-6] antiviral,[7-8] anticonvulsant,[9-10] and antidiabetic activities.[11] In particular, owing to its versatility, fused 1,2,4-triazoles, which are incorporated with one or more heterocyclic moieties such as pyridine, pyridazine, pyrazole, and imidazole rings, have received mounting research interest over the past decade. Very commonly, the significance of these fused heterocyclic systems is reflected in several therapeutic applications, manifested through antifungal,[12] antitumor,[13] cytotoxic,[14] antitubercular,[15] antiviral,[16] anticonvulsant,[17] and antimigraine[18] and other biological activities.[19-21] In addition to that, the usefulness of the 1,2,4-triazole system has also been

This work is licensed under a CC BY 4.0 license.

extended across various domains, such as polymers, corrosion inhibitors, ionic liquids, agrochemicals, supramolecular chemistry, and materials science.[22-25] Pyridazine also represents a prominent class of six-membered aza-heterocyclic compounds containing two nitrogen and four carbon atoms. Consistent with 1,2,4-triazoles, pyridazine derivatives constitute valuable pharmacophores by virtue of their remarkable biological potential, exhibiting antimicrobial,[26] antiviral,[27] antitumor,[28] antitubercular,[29] and anticancer[30] activities. Notably, pyridazine rings fused with 1,2,4-triazole moieties (1,2,4-triazolopyridazine scaffolds) have been identified as ligands for the GABA receptor,[31] as agents showing activity against the Hepatitis A virus (HAV)[32] and as c-Met kinase inhibitors.[33] Interestingly, Schiff base triazoles are another type of ubiquitous derivatives, found to have remarkable activity like c-Met inhibitors,[34-35] antitumor,[36] antiviral,[37] antituberculosis,[38] antimalarial activities.[39] Some of the biologically important[1,2,4]triazolo[4,3-b]pyridazine analogues are shown in the Fig. 1.

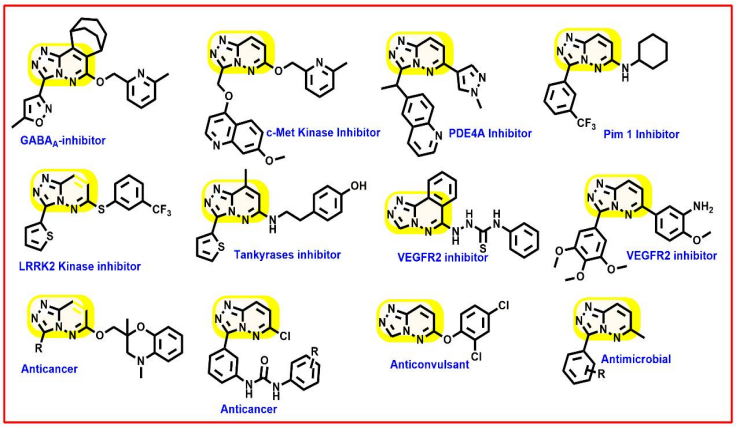

Fig.-1: Biologically Important [1,2,4]triazolo[4,3-*b*]pyridazine Molecules

Abnormal regulation of Wnt/β-catenin signalling has been well reported as an important contributor to the initiation and progression of human cancers.[40] Several biological processes, including cell proliferation, differentiation, migration, stem cell maintenance, and tissue homeostasis, have been affected by the disruption of this pathway, leading to tumorigenesis. Also, it has been demonstrated that the abnormality of Wnt/β-catenin signalling results in various human malignancies, with prominent involvement in colorectal, liver, breast, and lung cancers. Considering this pathway of Wnt signalling, β-catenin has been widely accepted as a privileged target for drug discovery. Although numerous studies have confirmed the biological significance of 1,2,4-triazolopyridazine scaffolds, only a limited number of reports have described an integrated approach combining antimicrobial evaluation with computational studies.[41-45] Therefore, motivated by these findings, eleven novel Schiff bases (5a–5k) were synthesised and evaluated for their antimicrobial activity. In addition, *in silico* molecular docking studies were performed to investigate their preliminary binding affinity with the β-catenin protein (PDB ID: 1JDH), using FH-535 as the reference inhibitor. Furthermore, toxicity prediction was carried out to examine the safety profile of the synthesised novel derivatives. This study supports United Nations Sustainable Development Goal 3 to develop and discover novel therapeutic drugs.

EXPERIMENTAL

Materials and Methods

The chemicals involved for the synthesis were procured from appropriate suppliers and used directly unless otherwise specified. Melting points of 5a–5k were checked using a B-545 apparatus. A JEOL 600 MHz NMR spectrometer (JEOL, Japan) was used to record the ^{1}H NMR and ^{13}C NMR spectra. Tetramethylsilane (TMS) served as the internal standard, while DMSO-d$_6$ was served as the deuterated solvent. The ^{13}C NMR spectra were acquired at 150 MHz. Molecular masses of the synthesised compounds were confirmed using an Agilent 1200 Series LC–MS system. TLC plate purchased from Merck was utilised for monitoring the reaction profile, and an ethyl acetate and hexane mixture (4:6) was used as an eluent. Purification of the isolated crude products was accomplished by silica gel column chromatography (230–400 mesh).

Synthetic Procedure for the Synthesis of 6-methyl-3-(3-nitrophenyl)-[1,2,4]triazolo[4,3-*b*]pyridazine (3)

A mixture of compound 1 (0.120 mol) and aldehyde 2 (0.142 mol) was dissolved in ethanol (150 mL) and refluxed under constant stirring for 2 h. The formation of the product was periodically examined by thin-layer chromatography (TLC). After the starting materials had been completely consumed, the reaction mixture was allowed to reach room temperature. Water (15 mL) was then introduced, and the mixture was heated again to 60–65 °C. Phenyliodine (III) diacetate [$PhI(OAc)_2$] (0.161 mmol) was subsequently added in ten equal portions over 20–30 min while maintaining the reaction temperature within 60–65 °C. Stirring was continued at the same temperature for a further 3 h. Once the reaction was complete, the mixture was cooled to 10–15 °C and maintained at this temperature under stirring for 45 min. The pale-yellow solid that separated was isolated by vacuum filtration, the solid was washed thoroughly with water, and dried under reduced pressure to afford compound **3**.

Synthetic Procedure for the Synthesis of 3-(6-methyl-[1,2,4]triazolo[4,3-*b*]pyridazin-3yl)aniline (4)

Compound 3 (0.390 mol) was suspended in methanol (100 mL) together with activated carbon (2.0 g, 20 wt.%) and anhydrous $FeCl_3$ (6 wt.%). The reaction mixture was heated to 50–55 °C, after which hydrazine hydrate (20 mL) was added slowly while maintaining the same temperature. Upon completion of the addition, the reaction was allowed to proceed at 50–55 °C until thin-layer chromatography (TLC) confirmed complete consumption of the starting material. The mixture was subsequently cooled to room temperature and filtered through a Celite pad to remove the insoluble materials. The resulting filtrate was concentrated under reduced pressure to furnish compound 4 as an off-white solid.

General Procedure for Synthesis of N-benzylidene-3-(6-methyl-[1,2,4]triazolo[4,3-*b*]pyridazin-3-yl)aniline Derivatives (5a-5k)

Compound **4** (0.002 mol) and the appropriate arylaldehyde (0.003 mol) were dissolved in ethanol (20 mL), and the resulting solution was refluxed under continuous stirring for 2 h. The progress of the reaction was monitored periodically by thin-layer chromatography (TLC) until complete consumption of the starting material was observed. The reaction mixture was then allowed to cool and subsequently maintained at 10–15 °C for 45 min to promote crystallisation. The separated solid was isolated by filtration and dried to afford the desired N-benzylidene derivatives (5a–5k).

3-(6-methyl-[1,2,4]triazolo[4,3-b]pyridazin-3yl)aniline (4)

Off white solid; 80 %; Mp: 120 °C ^{1}H NMR (600 MHz, DMSO-d_6): δ = 2.64 (s, 3H, CH_3), 5.8 (br, 2H, -NH_2), 7.30-7.28 (m, 2H, ArH), 7.48-7.46 (m, 1H, ArH), 7.80-7.78 (m, 2H, ArH), 7.97 (s,1H, ArH): ^{13}C NMR (150 MHz, DMSO-d_6): δ = 21.6, 118.6, 120.6, 120.9, 122.1, 122.2, 123.8, 125.2, 127.5, 131.1, 145.6, 154.7; Anal. calcd. For $C_{12}H_9N_5O_2$: C, 56.47; H, 3.55; N, 27.44; Found: C, 56.53; H, 3.60; N, 27.51; LC-MS: (*m/z*) calcd for $C_{12}H_9N_5O_2$ $[M+H]^+$ 256.23; observed: 256.

N-**(2-bromobenzylidene)-3-(6-methyl-[1,2,4]triazolo[4,3-*b*]pyridazin-3-yl)aniline (5a)**

White solid; 74 %; Mp: 184–186 °C; ^{1}H NMR (600 MHz, DMSO-d_6): δ= 2.62 (s, 3H -CH_3), 7.33-7.25 (m, 2H, ArH), 7.52-7.46 (m, 3H, ArH), 7.26-7.24 (m, 2H, ArH), 7.43 (s, 1H, ArH), 8.29-8.27 (d, J = 5.2 Hz, 1H, ArH), 8.30 (m, 1H, ArH), 8.65 (s, 1H, CH=N); ^{13}C NMR (150 MHz, DMSO-d_6) δ= 21.2, 121.5, 121.9, 123.3, 125.8, 126.2, 127.1, 127.3, 127.5, 130.3, 130.5, 131.1, 132.5, 135.1, 143.2, 150.0, 153.6, 159.2, 158.9; Anal. calcd for $C_{19}H_{14}BrN_5$: C, 58.18; H, 3.60; N, 17.85. Found: C, 58.30; H, 3.82; N, 17.90; LC-MS: (*m/z*) calcd for $C_{19}H_{14}BrN_5$ $[M+H]^+$ 393.25; observed: 393.

N-**(2-fluorobenzylidene)-3-(6-methyl-[1,2,4]triazolo[4,3-*b*]pyridazin-3-yl)aniline (5b)**

White solid; 76 %; Mp: 165–167 °C; ^{1}H NMR (400 MHz, DMSO-d_6): δ= 2.65 (s, 3H -CH_3), 7.37-7.35 (m, 2H, ArH), 7.67- 7.65 (m, 2H, ArH), 8.16 (s, 1H, ArH), 8.31-8.30 (m, 3H, ArH), 8.74 (s, 1H, ArH), 8.30 (m, 1H, ArH), 8.65 (s, 1H, CH=N); ^{13}C NMR (150 MHz, DMSO-d_6) δ= 20.8, 114.6, 118.5, 121.5, 122.1, 123.1, 124.0, 127.1, 126.3, 130.3, 130.5, 131.4, 132.2, 143.2, 150.9, 153.2, 158.8, 159.4 160.0; Anal. calcd for $C_{19}H_{14}FN_5$: C, 68.87; H, 4.26; N, 21.14: Found: C, 68.92; H, 4.31; N, 21.19; LC-MS: (*m/z*) calcd for $C_{19}H_{14}FN_5$ $[M+H]^+$ 333.35; observed: 332.

Methyl4-(((3-(6-methyl-[1,2,4]triazolo[4,3-*b*]pyridazin-3-yl)phenyl)imino)methyl)benzoate (**5c**) Off white solid; 74 %; Mp: 192–194 °C; ^{1}H NMR (600 MHz, DMSO-d_6): δ= 2.63 (s, 3H -CH_3), 3.35 (s, 3H, OCH_3), 7.25- 7.24 (d, 1H, J = 10.2 Hz, ArH), 7.33-7.32 (dd, 2H, J = 7.8 Hz, ArH), 7.47 (s, 1H, ArH), 7.73 (s, 1H, ArH), 7.80 (s, 1H, ArH), 7.92-7.87 (m, 2H, ArH), 8.05 (s, 1H, CH=N), 8.34-8.32 (dd, 2H, J = 7.8 Hz, ArH); ^{13}C NMR (150 MHz, DMSO-d_6) δ= 21.2, 88.2, 113.5, 118.7, 123.3, 124.7, 124.9, 125.2, 128.0, 128.1 130.0, 132.2, 134.9, 144.7, 146.0, 146.1, 146.2, 155.8, 169.6; Anal. calcd for $C_{21}H_{17}N_5O_2$: C, 67.91; H, 4.61; N, 18.86; Found: C, 68.03; H, 4.71; N, 18.92; LC-MS: (*m/z*) calcd for $C_{21}H_{17}N_5O_2$ $[M+H]^+$ 372.39; observed: 372.

N,N-dimethyl-4-(((3-(6-methyl-[1,2,4]triazolo[4,3-b]pyridazin-3-yl)phenyl)imino)methyl)aniline (**5d**) White solid; 80 %; Mp: 174–176 °C; ^{1}H NMR (600 MHz, DMSO-d_6): δ= 2.63 (s, 3H -CH_3), 3.05 (s, 6H, N-(CH_3)2), 6.85- 6.79 (dd, 2H, d, J = 7.8 Hz, ArH), 7.41-7.28 (m, 2H, ArH), 7.76-7.62 (m, 1H, ArH), 7.87-7.77 (d, 2H, J = 7.8 Hz, ArH), 8.33-8.12 (m, 2H, ArH), 8.42-8.33 (m, 1H, ArH), 8.58 (s, 1H, CH=N); ^{13}C NMR (150 MHz, DMSO-d_6) δ= 21.2, 39.9, 119.1, 120.1, 122.8, 123.4, 124.1, 124.2, 125.0, 127.7, 130.2, 131.0, 144.8, 146.9, 151.1, 153.0, 153.2, 156.0, 161.3; Anal. calcd for $C_{21}H_{20}N_6$: C, 70.77; H, 5.66; N, 23.58: Found: C, 70.82; H, 5.76; N, 23.71; LC-MS: (*m/z*) calcd for $C_{21}H_{20}N_6[M+H]^+$ 357.42; observed: 357.

4-(Benzyloxy)benzylidene)-3-(6-methyl-[1,2,4]triazolo[4,3-*b*]pyridazin-3-yl)aniline (**5e**)
White solid; 78 %; Mp: 204–208 °C; ^{1}H NMR (600 MHz, DMSO-d_6): δ= 2.57 (s, 3H -CH_3), 5.23 (s, 2H, OCH_2-Ar), 7.19- 7.17 (d, 2H, J = 7.8 Hz, ArH), 7.36-7.34 (d, 2H, J = 7.2 Hz, ArH), 7.42-7.41 (m, 3H, ArH), 7.48-7.46 (m, 2H, ArH), 7.62-7.59 (m, 1H, ArH), 7.95-7.93 (d, 2H, J = 7.8 Hz, ArH), 8.22-8.16 (m, 1H, ArH), 8.27-8.24 (m, 1H, ArH), 8.41(m, 1H, ArH), 8.64 (s, 1H, CH=N); ^{13}C NMR (150 MHz, DMSO-d_6) δ= 21.4, 69.9, 115.7, 120.2, 123.5, 123.6, 125.05, 125.6, 127.8, 128.3, 128.5, 129.0, 130.3, 130.5, 131.2, 137.1, 144.8, 146.8, 152.6, 156.0, 161.3, 161.7; Anal. calcd for $C_{26}H_{21}N_5O$: C, 74.44; H, 5.05; N, 16.70; Found: C, 74.32; H, 5.10; N, 16.84; LC-MS: (m/z) calculated for $C_{26}H_{21}N_5O$ $[M+H]^+$ 420.48; observed: 420.

N-(4-(4-fluorophenoxy)benzylidene)-3-(6-methyl-[1,2,4]triazolo[4,3-*b*]pyridazin-3-yl)aniline(**5f**)
White solid; 83 %; Mp: 193–195 °C; ^{1}H NMR (600 MHz, DMSO-d_6): δ= 2.63 (s, 3H -CH_3), 7.36-7.34 (d, 2H, J = 7.2 Hz, ArH), 7.49-7.47 (m, 2H, ArH), 7.48-7.46 (m, 2H, ArH), 7.85-7.83 (m, 2H, ArH), 7.98-7.95 (d, 2H, J = 7.8 Hz, ArH), 8.24-8.21 (m, 1H, ArH), 8.33-8.29 (m, 1H, ArH), 8.37-8.33 (m, 2H, ArH), 8.76 (s, 1H, CH=N); ^{13}C NMR (150 MHz, DMSO-d_6) δ= 22.1, 120.4, 123.0, 123.5, 125.0, 126.6, 127.9, 129.0, 130.4, 130.6, 130.8, 131.7, 132.0, 132.3, 134.6, 136.9, 144.8, 146.6, 151.5, 156.1, 151.9; Anal. calcd for $C_{25}H_{18}FN_5O$: C, 71.38; H, 4.61; N, 16.01; Found: C, 71.45; H, 4.61; N, 16.10; LC-MS: (m/z) calcd for $C_{25}H_{18}FN_5O$ $[M+H]^+$ 424.44; observed: 424.

N-(2,6-dibromobenzylidene)-3-(6-methyl-[1,2,4]triazolo[4,3-*b*]pyridazin-3-yl)aniline(**5g**)
White solid; 80 %; Mp: 210–214 °C; ^{1}H NMR (600 MHz, DMSO-d_6): δ= 2.63 (s, 3H -CH_3), 7.36-7.34 (d, 1H, J = 9.6 Hz, ArH), 7.50-7.49 (d, 1H, J = 7.2 Hz, ArH), 7.69-7.67 (m, 1H, ArH), 7.74-7.73 (d, 2H, J = 8.4 Hz, ArH), 8.25 (s, 1H, ArH), 8.35-8.33 (m, 3H, ArH), 8.83 (s, 1H, CH=N); ^{13}C NMR (150 MHz, DMSO-d_6) δ= 22.1, 119.7, 121.8, 123.5, 124.7, 125.0, 126.0, 128.0, 130.5, 131.5, 135.8, 136.2, 144.9, 146.5, 151.2, 156.0, 158.7; Anal. calcd for $C_{19}H_{13}Br_2N_5$: C, 48.44; H, 2.78; N, 14.86; Found: C, 48.48; H, 2.82; N, 14.92; LC-MS: (m/z) calcd for $C_{19}H_{13}Br_2N$ $[M+H]^+$ 472.15; observed: 472.

N-(2,6-dichlorobenzylidene)-3-(6-methyl-[1,2,4]triazolo[4,3-b]pyridazin-3-yl)aniline(**5h**)
White solid; 81 %; Mp: 220–222 °C; ^{1}H NMR (600 MHz, DMSO-d_6): δ= 2.62 (s, 3H -CH_3), 7.36-7.33 (d, 1H, J = 9.5 Hz, ArH), 7.48-7.46 (d, 1H, J = 7.2 Hz, ArH), 7.68-7.66 (m, 1H, ArH), 7.74-7.72 (d, 2H, J = 8.4 Hz, ArH), 8.27 (s, 1H, ArH), 8.36-8.34 (m, 3H, ArH), 8.94 (s, 1H, CH=N); ^{13}C NMR (150 MHz, DMSO-d_6) δ= 22.1, 119.6, 122.7, 123.5, 124.7, 125.0, 125.7, 128.0, 129.7, 130.5, 132.5, 134.5, 144.9, 146.4, 151.7, 156.0, 158.4; Anal. calcd for $C_{19}H_{13}Cl_2N_5$: C, 59.70; H, 3.43; N, 18.32 Found: C, 59.75; H, 3.48; N, 18.38; LC-MS: (m/z) calcd for $C_{19}H_{13}Cl_2N_5$ $[M+H]^+$ 383.25; observed: 383.

N-(2-bromo-4-methoxybenzylidene)-3-(6-methyl-[1,2,4]triazolo[4,3-b]pyridazin-3-yl)aniline(**5j**)
White solid; 85 %; Mp: 174–176 °C; ^{1}H NMR (600 MHz, DMSO-d_6): δ= 2.61 (s, 3H -CH_3), 3.90 (s, 3H -

OCH_3), 7.24-7.23 (d, 2H, J = 9.0 Hz, ArH), 7.44-7.40 (m, 2H, ArH), 7.83-7.81 (m, 3H, ArH), 8.27-8.26 (d, 2H, J = 1.2 Hz, ArH), 8.92 (s, 1H, CH=N); ^{13}C NMR (150 MHz, DMSO-d_6) δ= 22.2, 56.9, 116.0, 119.7, 123.3, 123.5, 125.0, 125.4, 126.1, 127.8, 129.4, 130.4, 136.1, 139.0, 144.8, 152.2, 155.5, 156.0, 159.0, 161.0: Anal. calcd for $C_{20}H_{16}BrN_5O$: C, 56.89; H, 3.82; N, 16.58; Found: C, 56.92; H, 3.88; N, 16.63; LC-MS: (m/z) calcd for $C_{20}H_{16}BrN_5O[M+H]^+$ 423.28; observed: 423.

N-((5-bromopyridin-2-yl)methylene)-3-(6-methyl-[1,2,4]triazolo[4,3-b]pyridazin-3-yl)aniline(5k)
Pale yellow solid; 79 %; Mp: 216–218 ºC; ^{1}H NMR (600 MHz, DMSO-d_6): δ= 2.65 (s, 3H -CH_3), 6.73-6.72 (m, 1H, ArH), 7.37-7.35 (m, 1H, ArH), 7.69 (s, 1H, ArH), 8.22-8.15 (m, 1H, ArH), 8.22-8.20 (m, 1H, ArH), 8.35-8.33 (m, 3H, ArH), 8.68 (s, 1H, ArH), 8.90 (s, 1H, CH=N); 13C NMR (150 MHz, DMSO-d_6) δ= 22.1, 120.7, 122.8, 123.1, 123.7, 125.0, 126.0, 127.9, 129.7, 130.5, 144.9, 146.6, 151.1, 151.6, 153.0, 156.0, 159.0, 161.0 Anal. calcd for $C_{18}H_{13}BrN_6$: C, 54.98; H, 3.33; N, 21.37; Found: C, 54.78; H, 3.40; N, 21.39; LC-MS: (m/z) calcd for $C_{18}H_{13}BrN_6$ $[M+H]^+$ 394.24; observed: 394.

Antimicrobial Studies
All eleven targeted molecules (5a–5k) were employed to evaluate their antimicrobial efficacy against Gram-positive bacterial strains, namely *Staphylococcus aureus* and *Bacillus subtilis*; Gram-negative bacterial strains, including *Escherichia coli* and *Pseudomonas aeruginosa*; as well as the fungal strains *Aspergillus flavus* and *Aspergillus niger*. Bacterial and fungal cultures were grown on nutrient agar and dextrose agar plates, respectively. All eleven derivatives and the standard drugs were dissolved in DMSO and placed into the wells at a 150 μg mL^{-1} concentration. Ampicillin and fluconazole were chosen as the standard antibacterial and antifungal agents, respectively.

Docking Studies
Computer-aided molecular docking analysis of 5a–5k molecules was performed using the Swiss Dock web server tool,[46] and visualisation of the docked conformations was carried out using BIOVIA Discovery Studio Visualizer 4.0.[47] Protein-ligand binding affinity and interaction profiles of the eleven compounds (5a-5k) were systematically analysed and compared with reference inhibitor FH-535. Initially, the resolved β-catenin X-ray structure (PDB ID: 1JDH) was taken from the Protein Data Bank. Before docking, irrelevant molecules, such as crystal-derived water molecules and heteroatomic residues, were removed from the protein structure, followed by hydrogen addition and energy minimisation. The prepared protein (β-catenin; PDB ID: 1JDH) was subsequently uploaded to the Swiss Dock web server for docking analysis. Both the reference inhibitor (FH-535) and the novel derivatives (5a–5k) were individually docked into the active site of β-catenin using identical docking parameters (box size: 20 × 20 × 20; box centre: −8.0, 9.0, 47.0). For each ligand, several binding poses were computed, and the lowest-energy conformer was selected for further analysis.

Toxicity Prediction
Toxicity is one of the most critical parameters in drug discovery programs, as it determines whether a substance is a potent therapeutic. For this purpose, the toxicity profile of the newly derived compounds (5a-5k) was predicted using ProTox-3.0. This platform provides comprehensive information on multiple toxicity endpoints based on the molecule profiles. The SMILES notations of selected compounds (5e, 5f, 5g, and 5h), along with the reference compound FH-535, were subjected to *in silico* toxicity evaluation. Toxicity assessment was performed for those selected compounds by examining organ-related adverse effects, including hepatic and cardiac toxicity, together with toxicological parameters such as carcinogenic potential, mutagenicity, cytotoxicity, and the blood–brain barrier permeability. In addition, the interactions of the selected compounds with Tox21 nuclear receptor and stress response pathways, as well as cytochrome P450 isoenzymes (CYP2C9, CYP2D6, and CYP3A4), were evaluated. The predicted active/inactive outcomes and their associated probability scores were subsequently compared with those of the reference inhibitor FH-535 to estimate the safety and drug-likeness of compounds (5a-5k).

RESULTS AND DISCUSSION
The method adopted to derive the eleven novel triazolo[4,3-*b*]pyridazine derivatives (5a–5k) was outlined in Scheme-1. As shown in Scheme-1, intermediate 3a was obtained by heating compounds 1 and 2 under

reflux in ethanol for 2 h. Without isolation, intermediate 3a was treated with water and Iodobenzene diacetate at refluxing temperature (60–65 °C) for 3 h, furnishing compound (3), which was subsequently reduced using hydrazine hydrate in the presence of activated charcoal and neutral ferric chloride in methanol under heating at 55-60 °C for 2 h to afford the corresponding aniline derivatives (4). Finally, condensation of intermediate 4 with aryl aldehydes having either electron-donating or electron-withdrawing functional groups in ethanol under reflux afforded 5a–5k (Table-1).

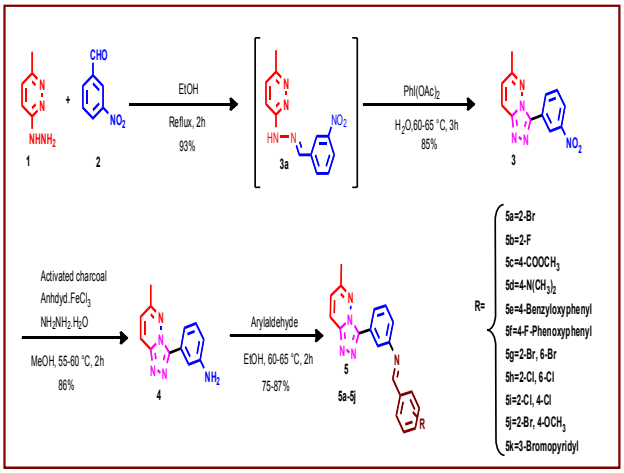

Scheme-1: Synthesis of N-benzylidene-3-(6-methyl-[1,2,4]triazolo[4,3-*b*]pyridazin-3-yl)aniline

Table-1: Structure of the Synthesised (5a–5k) Schiff base derivatives

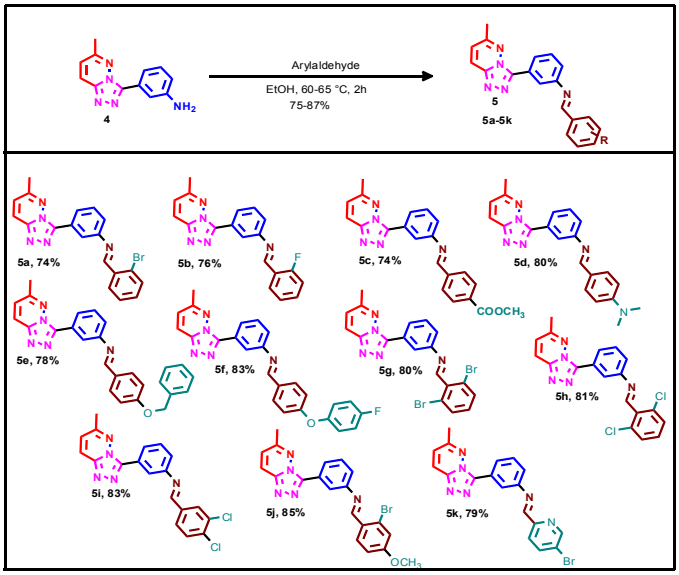

Antibacterial Activity

All the eleven Schiff base derivatives (5a–5k) were subjected to antimicrobial screening against representative Gram-positive and Gram-negative bacterial strains, and the obtained results are summarised in Table-2. Overall, the majority of the novel frameworks (5a-5k) displayed moderate to appreciable antibacterial activity against both bacterial strains. Among the Gram-positive bacteria, derivatives 5b, 5e, 5g, and 5h produced pronounced inhibitory effects against *Staphylococcus aureus* (11–12 mm) and *Bacillus subtilis* (10–12.5 mm), whereas the remaining derivatives exhibited comparatively lower activity. Of these, compound 5e showed the greatest inhibitory effect against *B. subtilis* (12.5 mm), approaching the activity of the reference drug ampicillin. Against the Gram-negative bacterial strains, *Escherichia coli* and *Pseudomonas aeruginosa*, compounds 5c, 5f, 5h, and 5i demonstrated comparatively

stronger antibacterial effects. Among them, compound 5i showed the largest inhibition zone (11 mm), manifesting its promising antibacterial efficacy against Gram-negative organisms.

Table-2: Antimicrobial Activities of Synthesised (*5a–5k*) Schiff base derivatives

Compound	Microorganism and inhibition zone in mm (150 μg mL^{-1})					
	Gram-positive bacteria		Gram-negative bacteria		Fungi	
	S. aureus	*B. subtilis*	*E. coli*	*P. aerug.*	*A. flavus*	*A. niger*
5a	9	7	8	6	5	4
5b	11	8.5	7	6.5	6	7
5c	6	6	9	8	9	8
5d	8	7.5	8	7	5	6
5e	11	10.5	7.5	9	6	7
5f	10	12	9	7.5	8	8
5g	11	10	7	6	5	4
5h	12	12.5	9	8	8	5
5i	8	9	10	11	9	10
5j	7	6	8.5	7	5	8
5k	6	9	5	6	7	9
Ampicillin	13	14	12	12	NA	NA
Fluconazole	NA	NA	NA	NA	10	11

S. aureus: Staphylococcus aureus (ATCC 25923); B. subtilis: Bacillus subtilis (ATCC 6633); E. coli: Escherichia coli (ATCC 25922); P. aerug: Pseudomonas aeruginosa (ATCC 27853); A. flavus: Aspergillus flavus (ATCC 204304); A. niger: Aspergillus niger (ATCC 16404); NA: Not applicable.

Antifungal Activity

The antifungal potential of the eleven novel Schiff base hybrids (5a–5k) was tested against *Aspergillus flavus* and *Aspergillus niger*, and the results are presented in Table-2. Overall, several compounds exhibited appreciable antifungal activity against the tested fungal strains. Among the synthesised eleven derivatives, compound 5i demonstrated the strongest inhibitory effect against *A. niger*, with the closest inhibition zone to that of fluconazole. Compounds 5c, 5f, 5i, and 5k also showed moderate antifungal activity, producing inhibition zones ranging from 8 to 10 mm, whereas the remaining derivatives displayed relatively weak activity against both fungal species. The observed differences in antimicrobial activity among 5a–5k derivatives may be attributed to the inductive (+I and -I) and resonance (mesomeric) impact of the substituent groups present on the aromatic ring. Hence, the result supports the importance of the 1,2,4-triazole scaffold in the development of potent antimicrobial agents.

Docking Studies

The *in silico* screening results obtained from the molecular docking studies, including binding energy (ΔG), inhibition constant (Ki), ligand efficiency (LE), interacting amino acid residues, and the nature of molecular interactions, are presented in Table-3. Based on the calculated inhibition constants (Ki), the synthesised compounds (5a–5k) clearly demonstrated stronger binding affinity than the reference inhibitor FH-535. Among the docked compounds, 5e, 5f, 5g, and 5h showed the most remarkable docking scores (−7.01 to −7.71 kcal/mol) along with low estimated Ki values. Furthermore, the calculated ligand efficiency (LE) values ranged from 0.23 to 0.30, indicating good structural efficiency.

This indicates optimal utilisation of molecular size for effective binding. The stability of the complexes can be attributed to the strength of the non-covalent interactions of the ligands with various significant residues present in the binding cavity. Notably, residues such as ARG342, LYS345, TYR306, TRP383, VAL349, and VAL346 were consistently involved in interactions with the synthesised compounds. The formation of conventional hydrogen bonds together with hydrophobic contacts enhances stable ligand binding within the active site, resulting in favourable protein–ligand complex stability.

Furthermore, the incorporation of heterocyclic moieties in the synthesised derivatives is likely to promote their molecular recognition and contribute to their inhibitory activity. Overall, compounds 5e, 5f, 5g, and 5h exhibited superior binding interactions compared to the other synthesised derivatives as well as the reference ligand FH-535.

Table-3: Docking score of synthesised compounds (5a-5k) including their Inhibition Constant, Ligand Efficiency, Distance, Interacting Amino Acids and Type of Interactions

Compound	Binding Energy (ΔG = kcal mol^{-1})	Inhibition Constant (Ki, μM)	Ligand Efficiency (LE)	Distance (Å)	Interacting Residues	Type of Interaction
5a	-7.35	2.98	0.29	4.31; 3.87; 4.10; 3.77; 3.78; 4.30; 5.04; 4.94; 4.37	A:ARG342; A:LYS345; A:GLN302; A:VAL349; A:VAL346; A:TYR306; A:TRP383; A:ARG342; A:LYS345	π Cation; π- donor H; π– donor H; π– σ; Alkyl; π -Alkyl ; π-Alkyl ; π -Alkyl; π -Alky
5b	-7.48	3.20	0.30	2.28; 2.62; 4.72; 2.84; 5.56; 4.89; 4.87; 4.40; 5.20; 4.31	A:GLY307; A:TYR306; A:ARG342; A:LYS345; A:TYR306; A:TRP383; A:ARG342; A:LYS345; A:VAL346; A:VAL349	Convl. H- Bond; C-H; π Cation; π- donor H; π– donor H; π–π; π-Alkyl; π-Alkyl; π-Alkyl; π-Alkyl
5c	-7.18	5.38	0.29	2.42; 4.97; 2.46; 4.93; 4.40; 5.13; 5.09; 4.65; 4.66; 4.05; 4.96	A:ASN380; A:ARG342; A:LYS345; A:LYS345; A:TRP383; A:ARG342; A:LYS345; A:VAL346; A:VAL349; A:VAL349; A:VAL349	Convl. H- Bond; π Cation; π -Cation; π- donor H ; Alkyl; π-Alkyl; π-Alkyl; π-Alkyl; π-Alkyl; π-Alkyl; π-Alkyl
5d	-7.28	2.18	0.24	4.15; 4.88; 3.72; 5.31; 4.83; 5.10; 4.50; 4.90; 4.24;	A:LYS312; A:ARG342; A:LYS345; A:TYR306; A:TRP383; A:VAL346; A:VAL349; A:ARG342; A:LYS345	π -Cation; π- donor H; π -cation; π- donor H; π–π; π-Alkyl; π-Alkyl; π-Alkyl; π-Alkyl; π-Alkyl
5e	-7.71	2.18	0.24	3.36; 3.81; 3.69; 3.96; 3.73; 5.19; 4.35	A:LYS312; A:LYS312; A:LYS345; A:VAL349; A:VAL349; A:TYR306 ; A:LYS34	Convl. H- Bond; π -Cation; π- donor H; π -Cation; π- donor H; π– σ; π– σ; π–π; π-Alkyl
5f	-7.60	2.65	0.23	3.61; 4.54; 3.99; 4.28; 2.90; 5.38; 4.96; 4.72; 5.04; 4.25; 4.46	A:GLN309; A:LYS312; A:LYS312; A:ARG342; A:LYS345; A:TYR306; A:TRP383; A:VAL349; A:ARG342; A:LYS345; A:VAL349	Halogen (Fluorine); π -Cation; π -Cation; π -Cation; π -Cation; π- donor H; π–π; π-Alkyl; π-Alkyl; π-Alkyl; π-Alkyl; π-Alkyl
5g	-7.52	3.02	0.26	3.54; 4.43; 3.82; 4.15; 3.81; 3.71; 4.77; 4.16; 4.97; 5.09; 4.23	A:LYS345; A:ARG342; A:LYS345; A:GLN302; A:VAL349; A:VAL346; A:LYS345; A:TYR306; A:TRP383; A:ARG342; A:LYS345	H-donor; π -Cation; π -Cation; π- donor H; π- donor H; π– σ; Alkyl; Alkyl; π-Alkyl; π-Alkyl; π-Alkyl; π-Alkyl
5h	-7.68	2.33	0.30	2.62; 4.43; 2.87 4.65; 5.27; 5.01; 4.92; 4.33 ;4.00	A:LYS345; A:ARG342; A:LYS345; A:LYS345; A:VAL349; A:TRP383; A:ARG342; A:LYS345; A:VAL349	Donor -H; π -Cation; π -Cation; π- donor H; Alkyl; Alkyl; π-Alkyl; π-Alkyl; π-Alkyl; π-Alkyl
5i	-7.32	4.28	0.28	4.27; 4.17; 3.85; 3.56; 5.43; 4.21; 5.44; 5.14; 4.71; 4.92; 4.62; 5.43	A:ARG342; A:LYS345; A:ARG342; A:VAL349; A:TRP338; A:TRP383; A:TRP383; A:VAL349; A:VAL346; A:VAL349; A:ARG342; A:LYS345	π -Cation; π -Cation; π- donor H; π- donor; π– σ; π-Alkyl; π-Alkyl; π-Alkyl; π-Alkyl; π-Alkyl; π-Alkyl; π-Alkyl; π-Alkyl
5j	-7.30	4.17	0.26	4.17; 4.85; 3.77; 5.43; 4.71; 4.53; 4.83; 5.12; 4.39 4.87; 4.34	A:LYS312; A:ARG342; A:LYS345; A:TYR306; A:LYS345; A:VAL349 A:TRP383; A:VAL346; A:VAL349; A:ARG342; A:LYS345	π -Cation; π- donor H; π -Cation; π -Cation; π- donor H; π–π; Alkyl; Alkyl; π-Alkyl; π-Alkyl; π-Alkyl; π-Alkyl; π-Alkyl
5k	-7.01	7.20	0.27	4.63; 4.88; 4.38; 4.05; 4.92; 5.42; 4.13	A:ARG342; A:ARG342; A:LYS345; A:VAL349; A:TRP383; A:VAL346 A: VAL349	π -Cation; Alkyl; Alkyl; Alkyl; π-Alkyl; π-Alkyl; π-Alkyl; π-Alkyl
Reference (FH-535)	-5.45	100.41	0.17	3.26; 3.26; 3.47; 3.76; 4.97; 5.11; 4.87; 4.80	A:ARG342; A:LYS345; A:VAL346; A:LYS345; A:TYR306; A:ARG376 A:TRP383; A:LYS345	Convl. H- Bond; Convl. H- Bond; Convl. H- Bond; π -Cation; π- donor H; π -Cation; π–π; Alkyl; π-Alkyl; π-Alkyl

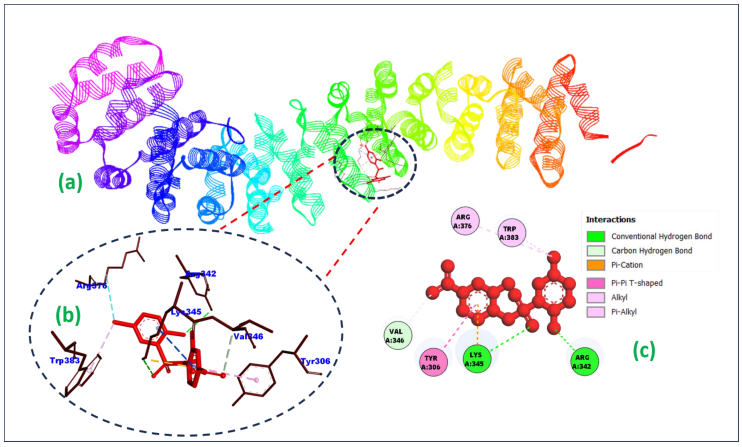

Fig.-2: Line Ribbon-3D (a) and 2D (b) Representation of FH-535 (reference ligand) binding interactions with β-Catenin (PDB: 1JDH)

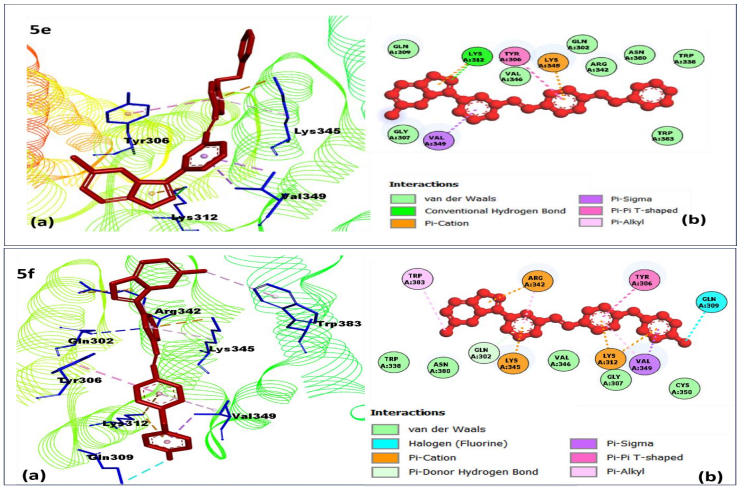

Fig.-3: 3D (a) and 2D (b) Representation of 5e and 5f Binding Interactions with β-catenin (PDB: 1JDH) (Continued)

Overall, these results suggest that the synthesised compounds warrant further biological investigation and lead optimisation. All eleven derivatives (5a-5k) demonstrated more favourable binding free energies (−7.01 to −7.71 kcal/mol) than the reference inhibitor FH-535, suggesting a favourable and strong affinity with stable occupancy of the β-catenin active site (Figs.-2 and 3). Therefore, the docking study suggests that β-catenin could serve as a remarkable molecular target for the selected scaffolds. However, further *in vitro* and *in vivo* investigations are required to evaluate this mechanism of action.

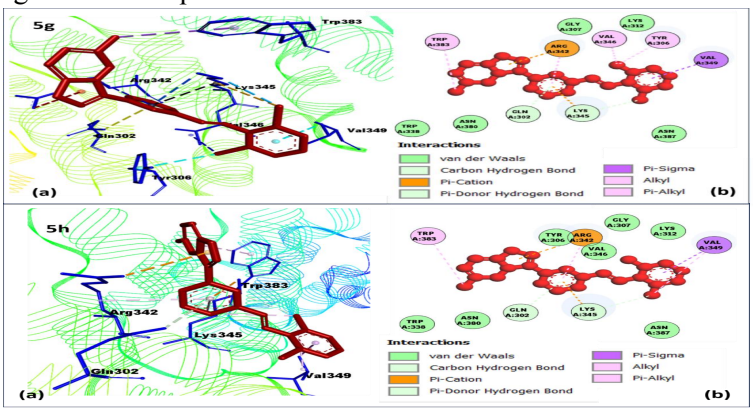

Fig.-3: 3D (a) and 2D (b) Representation of 5g and 5h Binding Interactions with β-catenin (PDB: 1JDH)

Toxicity Prediction

All the selected novel motifs were evaluated for their toxicity profiles using the ProTox-3.0 online tool, and the obtained values were analysed in comparison with the reference inhibitor, FH-535. This computational study was exclusively carried out to screen the toxicity prediction on organ toxicity, toxicity endpoints, nuclear receptor signalling, stress response pathways, and cytochrome P450 metabolism. As per the computed results, a favourable organ toxicity profile was found to be present in most of the selected compounds. (Figs.-4 and 5). The predicted toxicity profiles of the selected compounds and reference compounds are presented in Table-4.

Table-4: Predicted Toxicity Profile of the Selected Compounds and Reference Drugs/Inhibitor (toxicity probabilities shown in parentheses)

Comp.	Hepto.	Cardi.	Carci.	Muta.	Cyto.	BBB-b	Ahr	PPAR-G	MMP	p53	CYP2C9	CYP2D6	CYP3A4	Pre.LD_{50}
5e	0.53 (Inactive)	0.78 (Inactive)	0.56 (Inactive)	0.60 (Inactive)	0.73 (Inactive)	0.86 (Active)	0.57 (Active)	0.95 (Inactive)	0.77 (Inactive)	0.86 (Inactive)	0.51 (Active)	0.52 (Inactive)	0.53 (Inactive)	1000 mg/Kg
5f	0.59 (Active)	0.80 (Inactive)	0.66 (Inactive)	0.64 (Inactive)	0.62 (Inactive)	0.87 (Active)	0.50 (Active)	0.92 (Inactive)	0.64 (Inactive)	0.79 (Inactive)	0.55 (Active)	0.52 (Inactive)	0.59 (Inactive)	1000 mg/Kg
5g	0.59 (Active)	0.89 (Inactive)	0.69 (Inactive)	0.67 (Inactive)	0.78 (Inactive)	0.92 (Active)	0.61 (Active)	0.92 (Inactive)	0.78 (Inactive)	0.90 (Inactive)	0.55 (Active)	0.61 (Inactive)	0.59 (Inactive)	1000 mg/Kg
5h	0.52 (Active)	0.89 (Inactive)	0.72 (Inactive)	0.72 (Inactive)	0.83 (Inactive)	0.91 (Active)	0.61 (Active)	0.92 (Inactive)	0.80 (Inactive)	0.60 (Inactive)	0.65 (Active)	0.63 (Inactive)	0.59 (Inactive)	500 mg/Kg
Amp.	0.87 (Active)	0.82 (Inactive)	0.83 (Inactive)	0.94 (Inactive)	0.60 (Inactive)	1.00 (Active)	0.99 (Active)	0.99 (Inactive)	0.96 (Inactive)	0.99 (Inactive)	0.84 (Active)	0.97 (Inactive)	0.99 (Inactive)	5000 mg/Kg
Flu.	0.84 (Active)	0.79 (Inactive)	0.62 (Inactive)	0.52 (Inactive)	0.76 (Inactive)	0.96 (Active)	0.92 (Active)	0.99 (Inactive)	0.92 (Inactive)	0.97 (Inactive)	0.54 (Active)	0.50 (Inactive)	0.70 (Inactive)	1271 mg/Kg
FH-535	0.53 (Active)	0.64 (Inactive)	0.64 (Inactive)	0.62 (Inactive)	0.87 (Inactive)	0.74 (Active)	0.98 (Active)	0.94 (Inactive)	0.61 (Inactive)	0.87 (Inactive)	0.77 (Active)	0.65 (Inactive)	0.61 (Inactive)	132 mg/Kg

Hepto: Hepatotoxicity; Cardi: Cardiotoxicity; Carci: Carcinogenicity; Muta: Mutagenicity; Cyto: Cytotoxicity; mAhR: Aryl hydrocarbon Receptor; PPAR-Gamma: Peroxisome Proliferator Activated Receptor Gamma; MMP: mitochondrial Membrane Potential; p53: Phosphoprotein (Tumor Suppressor): CYP: Cytochrome P450; Amp: Ampicillin; Flu: Fluconazole

Compound 5f was predicted to be hepatotoxic and inactive for cardiotoxicity, whereas 5e, 5g, and 5h were projected to be inactive towards hepatotoxicity and cardiotoxicity. Considering the toxicity endpoints, the blood–brain barrier (BBB) permeability for the chosen scaffolds (5e, 5f, 5g, and 5h) was predicted to be active; conversely, all the hybrids were predicted to be non-carcinogenic, non-mutagenic, and non-cytotoxic. These results were comparable with the reference inhibitor FH-535. The compounds are also expected to have minimal CNS liability, as no signs of neurotoxicity were observed.

In addition, the selected compounds were found to have a low probability of receptor-mediated toxicity, comparable to or superior to the reference inhibitor. Based on the overall results, the synthesised compounds displayed an improved toxicity profile compared with the reference inhibitor FH-535, and the outcomes were comparable. In particular, the results related to mitochondrial stress response activation and nuclear receptor signalling interference support the newly synthesised compounds as potential lead candidates for antimicrobial and anticancer applications.

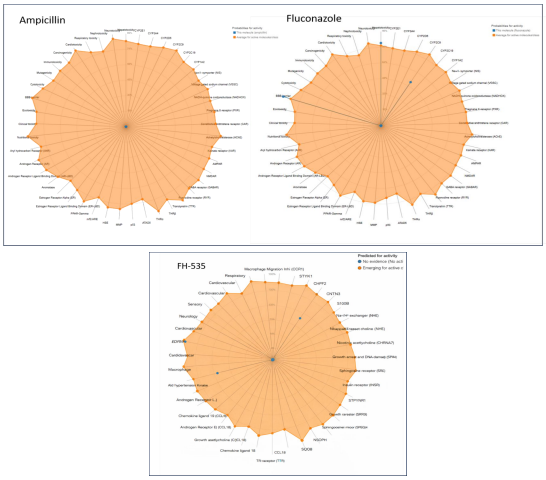

Fig.-4: Toxicity Radar: Ampicillin, Fluconazole, and FH-535

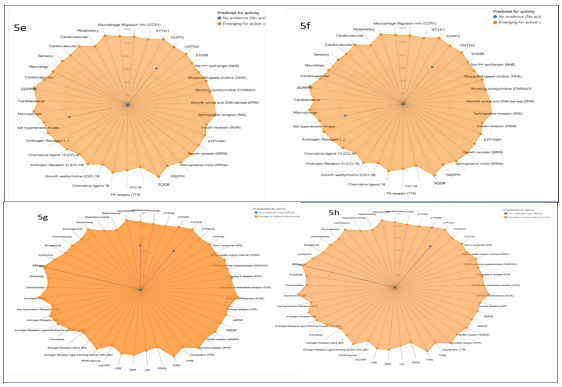

Fig.-5: Toxicity Radar of Selected Compounds (5e, 5f, 5g, and 5h)

CONCLUSION

In summary, a set of newly synthesised N-benzylidene-3-(6-methyl-[1,2,4]triazolo[4,3-*b*]pyridazin-3-yl)aniline derivatives (5a–5k) was constructed in order to perform antimicrobial screening, molecular docking, and computational toxicity assessment. The biological studies identified several derivatives with noteworthy antibacterial activity. Docking analysis indicated that the active compounds established favourable interactions within the β-catenin binding pocket, with some derivatives exhibiting higher predicted binding affinity than the reference ligand, FH-535. In addition, *in silico* toxicity evaluation suggested acceptable safety characteristics for the most active molecules. Based on the combined biological and computational findings, compounds 5e, 5f, 5g, and 5h were identified as the most promising candidates. These results demonstrate that the triazolo[4,3-b]pyridazine framework is a valuable structural platform for launching novel antimicrobial agents. Furthermore, the computational investigations provide an impetus for future experimental investigation to explore the interaction of these compounds with β-catenin and to assess their therapeutic potential. This contributes to ongoing efforts to address antimicrobial resistance and supports United Nations Sustainable Development Goal-3 (Good Health and Well-being) by promoting research toward safer and more effective therapeutic agents.

ACKNOWLEDGMENTS

The authors gratefully acknowledge the use of online computational and molecular modelling tools including BIOVIA Discovery Studio Visualizer, Swiss Dock, ProTox-II, and PyMOL for molecular docking, toxicity prediction, visualisation, and structural analysis studies carried out in this research work.

CONFLICT OF INTERESTS

The authors declare there are no conflicts of interest.

AUTHOR CONTRIBUTIONS

The present work is related to *SDG-3: Good Health and Well-being*. All the authors contributed significantly to this manuscript, participated in reviewing/editing and approved the final draft for publication. The research profile of the authors can be verified from their ORCID ids, given below:

N. Devika https://orcid.org/0009-0009-1004-7041
M. Mariyappan https://orcid.org/0000-0002-5647-4972
J. S. Ruso https://orcid.org/0009-0008-6891-3574
N. Sivakumar https://orcid.org/0009-0003-3469-4223
T. Anandarajan https://orcid.org/0009-0009-0311-1105

Open Access: This article is distributed under the terms of the Creative Commons Attribution 4.0 International License (http://creativecommons.org/licenses/by/4.0/), which permits unrestricted use, distribution, and reproduction in any medium, provided you give appropriate credit to the original author(s) and the source, provide a link to the Creative Commons license, and indicate if changes were made.
Cite this article as: N. Devika *et al.*, *Rasayan J. Chem.*, 19(4), 1948-1960(2026), https://doi.org/10.31788/RJC.2026.1949961

REFERENCES

1. E. Stingaci, M. Zveaghinteva, S. Pogrebnoi, *Bioorganic and Medicinal Chemistry Letters*, **30(17)**, 127368(2020), https://doi.org/10.1016/j.bmcl.2020.127368
2. S. P. Gami, P. T. Trivedi, M. D. Patel, S. B. Teraiya, F. G. Bhabhor, Y. T. Naliapara, *Rasayan Journal of Chemistry*, **19(1),** 511(2026), https://doi.org/10.31788/RJC.2026.1919482
3. S. Pokuri, R. Singla, V. Bhat, G. Shenoy, *Current Drug Metabolism*, **15(4)**, 389(2014), https://doi.org/10.2174/1389200215666140908101958
4. L. Perekhoda, V. Georgiyants, H. Yeromina and I. Drapak, *Chemistry and Chemical Technology*, **14(2)**, 214(2020), https://doi.org/10.23939/chcht14.02.214
5. O. Grytsai, O. Valiashko, M. Penco-Campillo, M. Dufies, A. Hagege, L. Demange, S. Martial, G. Pagès, C. Ronco, R. Benhida, *Bioorganic Chemistry*, **104**, 104271(2020) https://doi.org/10.1016/j.bioorg.2020.104271
6. H. S. Abulkhair, A. Turky, A. Ghiaty, H. E. A. Ahmed, A. H. Bayoumi, *Bioorganic Chemistry*, **100**, 103899(2020), https://doi.org/10.1016/j.bioorg.2020.103899
7. I. Küçükgüzel, E. Tatar, S. G. Küçükgüzel, S. Rollas, E. De Clercq, *European Journal of Medicinal* Chemistry, **43(2)**, 381(2008), https://doi.org/10.1016/j.ejmech.2007.04.010
8. A. Musa, H. S. Abulkhair, A. Aljuhani, N. Rezki, M. A. Abdelgawad, K. Shalaby, A. H. El-Ghorab, M. R. Aouad, *Pharmaceuticals*, **16(3),** 463(2023), https://doi.org/10.3390/ph16030463
9. B. Kaproń, R. Czarnomysy, M. Wysokiński, R. Andrys, K. Musilek, A. Angeli, C.T. Supuran, T. Plech, *Journal of Enzyme Inhibition and Medicinal Chemistry*, **35(1)**, 993(2020), https://doi.org/10.1080/14756366.2020.1748026
10. H. Abul-Khair, S. Elmeligie, A. Bayoumi, A. Ghiaty, A. El-Morsy, *Journal of Heterocyclic Chemistry*, **50**, 1202(2013), https://doi.org/10.1002/jhet.714
11. O. Abchir, M. Khedraoui, H. Nour, I. Yamari, A. Errouguiet, A. Samadi, S. Chtita, *Pharmaceuticals*, **17(2),** 261(2024), https://doi.org/10.3390/ph17020261
12. H. Miyauchi, K. Kozuki, T. Tanio, N. Ohashi, *Bioorganic and Medicinal Chemistry Letters*, **5(14)**, 1479(1995), https://doi.org/10.1016/0960-894X(95)00241-K
13. H. K. Nair, A. C. Peterson, P. T. Yazdi, R. Franzmair, *Bioorganic and Medicinal Chemistry Letters*, **7(18),** 2379(1997), https://doi.org/10.1016/S0960-894X(97)00433-2
14. A. T. Mavrova, D. Wesselinova, Y. A. Tsenov, P. Denkova, *European Journal of Medicinal Chemistry*, **44(1),** 63(2009), https://doi.org/10.1016/j.ejmech.2008.03.006
15. V. Klimešová, L. Zahajská, K. Waisser, J. Kaustová, U. Möllmann, Farmaco, **59(4),** 279(2004), https://doi.org/10.1016/j.farmac.2004.01.006
16. Y. Xia, Z. Fan, J. Yao, *Bioorganic and Medicinal Chemistry Letters*, **16(10)**, 2693(2006), https://doi.org/10.1016/j.bmcl.2006.02.023
17. J. M. Kane, M. A. Staeger, C. R. Dalton, *Journal of Medicinal Chemistry*, **37(1)**, 125(1994), https://doi.org/10.1021/jm00027a015
18. K. Wellington, G. L. Plosker, *Drugs*, **62**, 1539(2002), https://doi.org/10.2165/00003495-200262100-00007
19. S. Han, F. F. Zhang, X. Xie, J. Z. Chen, *European Journal of Medicinal Chemistry*, **74**, 73(2014), https://doi.org/10.1016/j.ejmech.2013.12.018
20. Y. S. Li, H. Tian, D. S. Zhao, *Bioorganic and Medicinal Chemistry Letters*, **26(15)**, 3632(2016), https://doi.org/10.1016/j.bmcl.2016.06.002
21. R. W. Carling, K. W. Moore, L. J. Street, *Journal of Medicinal Chemistry*, **47(7)**, 1807(2004), https://doi.org/10.1021/jm031020p
22. W. Zhang, J. Yuan, *Macromolecular Rapid Communications*, **37(23)**, 1124(2016), https://doi.org/10.1002/marc.201670092
23. N. P. Swathi, V. D. P. Alva, S. Samshuddin, *Journal of Bio- and Tribo-Corrosion*, **3**, 42(2017), https://doi.org/10.1007/s40735-017-0102-3
24. D. Caceres, C. Cebrian, A. M. Rodríguez, Chemical Communications, **49(6)**, 621(2013), https://doi.org/10.1039/C2CC37381E

25. L. D. Rodrigues, D. Sunil, D. Chaithra, *Journal of Molecular Liquids*, **297**, 111909(2020), https://doi.org/10.1016/j.molliq.2019.111909
26. F. A. Yassin, *Chemistry of Heterocyclic Compounds*, **45,** 997(2009), https://doi.org/10.1007/s10593-009-0381-9
27. J. Zhou, H. T. Fan, B. A. Song, L. Jin, P. S. Bhadury, D. Hu, S. Yang, *Phosphorus Sulfur and Silicon and the Related Elements*, **186(1)**, 81(2010), https://doi.org/10.1080/10426507.2010.482543
28. L. C. Bloomer, L. L. Wotring, L. B. Townsend, *Cancer Research*, **42**, 100(1982).
29. D. Mantu, M. C. Luca, C. Moldoveanu, *European Journal of Medicinal Chemistry*, **45(11)**, 5164(2010), https://doi.org/10.1016/j.ejmech.2010.08.029
30. W. Malinka, A. Redzicka, O. Lozach, *IL Farmaco*, **59(6)**, 457(2004), https://doi.org/10.1016/j.farmac.2004.03.002
31. L. J. Street, F. Sternfeld, R. A. Jelley, *Journal of Medicinal Chemistry*, **47(14)**, 3642(2004), https://doi.org/10.1021/jm0407613
32. A. H. Shamroukh, M. A. Ali, *Archiv der Pharmazie*, **341(4)**, 223(2008), https://doi.org/10.1002/ardp.200700181
33. B. K. Albrecht, J. C. Harmange, D. Bauer, *Journal of Medicinal Chemistry*, **51(10)**, 2879(2008), https://doi.org/10.1021/jm800043g
34. X. Liu, Y. Li, Q. Zhang, Q. Pan, P. Zheng, X. Dai, Z. Bai, W. Zhu, *Frontiers in Chemistry*, **10**, 815534(2022), https://doi.org/10.3389/fchem.2022.815534
35. Q. Zhang, X. Liu, W. Gan, J. Wu, H. Zhou, Z. Yang, Y. Zhang, M. Liao, P. Yuan, S. Xu, P. Zheng, W. Zhu, *ACS Omega*, **5(27)**, 16482(2020), https://doi.org/10.1021/acsomega.0c00838
36. X. Li, X. Q. Li, H. M. Liu, X. Z. Zhou, Z. H. Shao, *Bioorganic and Medicinal Chemistry Letters*, **22(2)**, 26(2012), https://doi.org/10.1093/nar/gkr366
37. A. R. Maarouf, A. A. Farahat, K. B. Selim, H. M. Eisa, *Medicinal Chemistry Research*, **21**, 703(2012), https://doi.org/10.1007/s00044-011-9574-8
38. P. A. Castelino, J. P. Dasappa, K. G. Bhat, S. A. Joshi, S. Jalalpure, *Medicinal Chemistry Research*, **25**, 83(2016), https://doi.org/10.1007/s00044-015-1461-2
39. S. S. Thakkar, P. Thakor, H. Doshi, A. Ray, *Bioorganic and Medicinal Chemistry*, **25**, 4064(2017), https://doi.org/10.1016/j.bmc.2017.05.054
40. S. Shang, F. Hua, Z. W. Hu, *Oncotarget*, **8**, 33972(2017), https://doi.org/10.18632/oncotarget.15687
41. G. Tian, Q. Song, Z. Liu, J. Guo, S. Cao, S. Long, *European Journal of Medicinal Chemistry*, **259**, 115603(2023), https://doi.org/10.1016/j.ejmech.2023.115603
42. M. Ajmal, A. K. Mahato, M. Khan, S. Rawat, A. Husain, E. B. Almalki, M. A. Alzahrani, A. Haque, M. J. Mohammed Hakme, A. S. Albalawi, M. Rashid, *Chemistry & Biodiversity*, **21(7)**, e202400637(2024), https://doi.org/10.1002/cbdv.202400637
43. M. U. Rehman, S. Long, *Future Medicinal Chemistry*, **16(23)**, 2451(2024), https://doi.org/10.1080/17568919.2024.2423596
44. W. Y. Belay, M. Getachew, B. A. Tegegne, Z. H. Teffera, A. Dagne, T. K. Zeleke, R. B. Abebe, A. A. Gedif, A. Fenta, G. Yirdaw, A. Tilahun, Y. Aschale, *Frontiers in Pharmacology*, **15**, 1444781(2024), https://doi.org/10.3389/fphar.2024.1444781
45. V. H. Krishnaprasad, S. Kumar, Journal of Medicinal Chemistry, **67(18)**, 15927(2024), https://doi.org/10.1021/acs.jmedchem.4c02002
46. A. Grosdidier, V. Zoete, O. Michielin, Nucleic Acids Research, **39(Suppl. 2)**, W270(2011), https://doi.org/10.1093/nar/gkr366
47. BIOVIA, Dassault Systèmes, *Discovery Studio Visualizer*, San Diego, CA, USA(2015)

[RJC-9961/2026]